Chemical Science

ROYAL SOCIETY OF CHEMISTRY

EDGE ARTICLE

View Article Online
View Journal | View Issue

Cite this: *Chem. Sci.*, 2023, **14**, 7980

All publication charges for this article have been paid for by the Royal Society of Chemistry

Received 16th May 2023
Accepted 28th June 2023

DOI: 10.1039/d3sc02474a

rsc.li/chemical-science

Catalytic asymmetric indolization by a desymmetrizing [3 + 2] annulation strategy†

Changhui Wu, [a] Zhiqian Chang,[a] Chuanyong Peng,[a] Chen Bai,[a] Junhao Xing[a] and Xiaowei Dou *[ab]

A new catalytic asymmetric indolization reaction by a desymmetrizing [3 + 2] annulation strategy is developed. The reaction proceeds *via* a rhodium-catalyzed enantioposition-selective addition/5-*exo*-trig cyclization/dehydration cascade between *ortho*-amino arylboronic acids and 2,2-disubstituted cyclopentene-1,3-diones to produce *N*-unprotected cyclopenta[*b*]indoles bearing an all-carbon quaternary stereocenter in high yields with good enantioselectivities. A quantitative structure–selectivity relationship (QSSR) model was established to identify the optimal chiral ligand, which effectively controlled the formation of the stereocenter away from the reaction site. Density functional theory (DFT) calculations, non-covalent interaction analysis, and Eyring analysis were performed to understand the key reaction step and the function of the ligand.

Introduction

Chiral indoles are ubiquitous in natural products, biologically active compounds, and functional molecules.[1,2] Continuous efforts have been devoted to developing efficient methods to access chiral indoles, and remarkable successes have been achieved in catalytic asymmetric transformations of indolyl substrates over the past decades.[3] Compared to asymmetric functionalization of indoles, asymmetric indolization represents a fundamentally different approach to chiral indoles by *de novo* construction of the indole ring. Therefore, it offers an irreplaceable tool to create novel chiral indole structures and to access otherwise difficult to prepare chiral indoles.[4] However, the lack of stereocenter in the indole ring can pose huge challenges for catalytic asymmetric indolization. In recent years, with the elegant design of substrate and reaction cascade, several catalytic asymmetric indolization reactions have been developed, which successfully addressed the challenges in asymmetric construction of axially chiral indoles.[5–8] In contrast, only a handful of examples have been disclosed for the synthesis of centrally chiral indoles *via* asymmetric indolization. One strategy is the asymmetric Fischer indolization developed by List group[9a] and Mukherjee group[9d] (Scheme 1a). Another strategy is the exquisitely designed asymmetric cascade reaction of 2-alkynyl aniline derivatives reported by Lu group[10a] and Zhu group[10b] among others[10] (Scheme 1b). Despite these elegant works, developing new strategies for asymmetric indolization to produce valuable chiral indoles is still highly desirable.[11]

Inspired by the Reissert indole synthesis,[12] which involves intramolecular dehydrating cyclization of the *in situ* generated β-aniline-substituted α-keto esters as the key step, we envisaged that an intermolecular [3 + 2] indolization reaction could be realized through cascade carbon–carbon bond formation/5-*exo*-trig cyclization/dehydration reaction between functionalized anilines and appropriate carbonyl substrates (Scheme 1c-top). When a prochiral carbonyl substrate was employed, the asymmetric [3 + 2] indolization shall be feasible. In light of our experience in asymmetric synthesis by rhodium-catalyzed conjugate addition of arylborons to α,β-unsaturated carbonyls,[13] we proposed to use *ortho*-amino arylborons under rhodium catalysis to construct the C–C bond,[14,15] and 2,2-disubstituted cyclopentene-1,3-diones[16] were selected as the prochiral carbonyl substrates. Ideally, the reactions between *ortho*-aminoarylborons and 2,2-disubstituted cyclopentene-1,3-diones could proceed *via* a conjugate addition/5-*exo*-trig cyclization/dehydration cascade to produce cyclopenta[*b*]indoles bearing an all-carbon quaternary stereocenter (Scheme 1c-middle).[17] In addition, the new strategy may overcome some limitations of the existing methods, such as the lengthy reaction time[9] and the tedious preparation of substrates.[10] However, there is a major challenge to be considered: the quaternary carbon stereocenter is away from the reaction site while the enantioselectivity is determined at the initial enantioposition-selective conjugate addition step (Scheme 1c-middle). Thus, the identification of a suitable catalyst that can effectively recognize the remote quaternary carbon stereocenter is crucial for the success of the asymmetric indolization.

[a]*Department of Chemistry, School of Science, China Pharmaceutical University, Nanjing, 211198, P. R. China. E-mail: dxw@cpu.edu.cn*

[b]*State Key Laboratory of Coordination Chemistry, Nanjing University, Nanjing, 210023, P. R. China*

† Electronic supplementary information (ESI) available: Experimental procedures, characterization, and computational details. CCDC 2260854 (for **3aa**). For ESI and crystallographic data in CIF or other electronic format see DOI: https://doi.org/10.1039/d3sc02474a

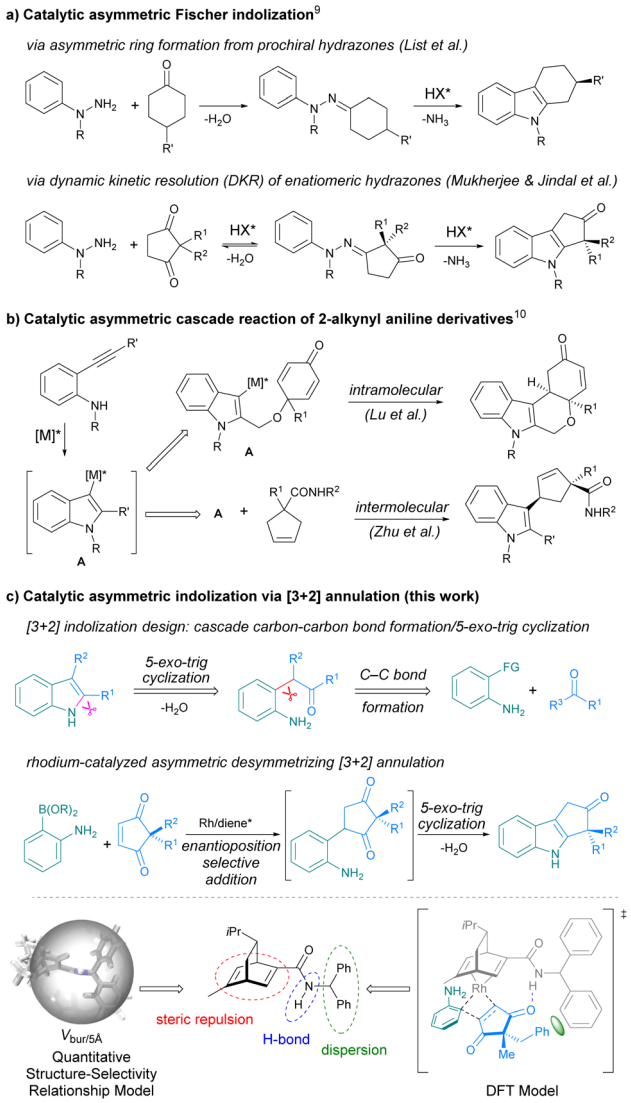

Scheme 1 Construction of centrally chiral indoles by catalytic asymmetric indolization.

Herein, we report a rhodium-catalyzed asymmetric indolization reaction *via* enantioposition-selective addition/5-*exo*-trig cyclization/dehydration cascade between *ortho*-aminoarylboronic acids and 2,2-disubstituted cyclopentene-1,3-diones, delivering *N*-unprotected cyclopenta[*b*]indoles bearing an all-carbon quaternary stereocenter in high yields with good to excellent enantioselectivities. The optimal chiral ligand that can effectively controls the remote quaternary carbon stereocenter was identified through a quantitative structure–selectivity relationship (QSSR) model, and the steric repulsion as well as the hydrogen bonding and dispersion interactions between the ligand and the substrate were found to collectively contribute to the high enantioselectivity (Scheme 1c-bottom).

Results and discussion

We initiated our investigation with 2-benzyl-2-methyl cyclopentene-1,3-dione **1a** and 2-aminophenylboronic acid **2a** as model substrates. After preliminary screening of the reaction conditions, it was found the reaction proceeded well in EtOH to give the indole product, and the chiral diene[18]-ligated rhodium catalysts gave promising results. As shown in Scheme 2, when using ester–diene ligands (L1, L2, and L3), the reaction exhibited promising enantioselectivities. Interestingly, the enantioselectivity of the reaction was improved when the corresponding amide–diene ligand was used (L1 *vs.* L4). Several other amide–diene[19] ligands were then tested. Intuitively, the enantioselectivity of the reaction increases with the size of the R group in the amide–diene ligands (R = Me, 89.5 : 10.5 er; R = *t*Bu, 93 : 7 er; R = 2,6-iPr$_2$C$_6$H$_3$, 95 : 5 er). Thus, a quantitative structure–selectivity relationship model was developed to understand this system (see ESI-Section 5† for details).[20] There is a linear correlation between the percent buried volume $V_{bur/5\text{ Å}}$ with a radius of 5 Å centered on the hydrogen atom of the

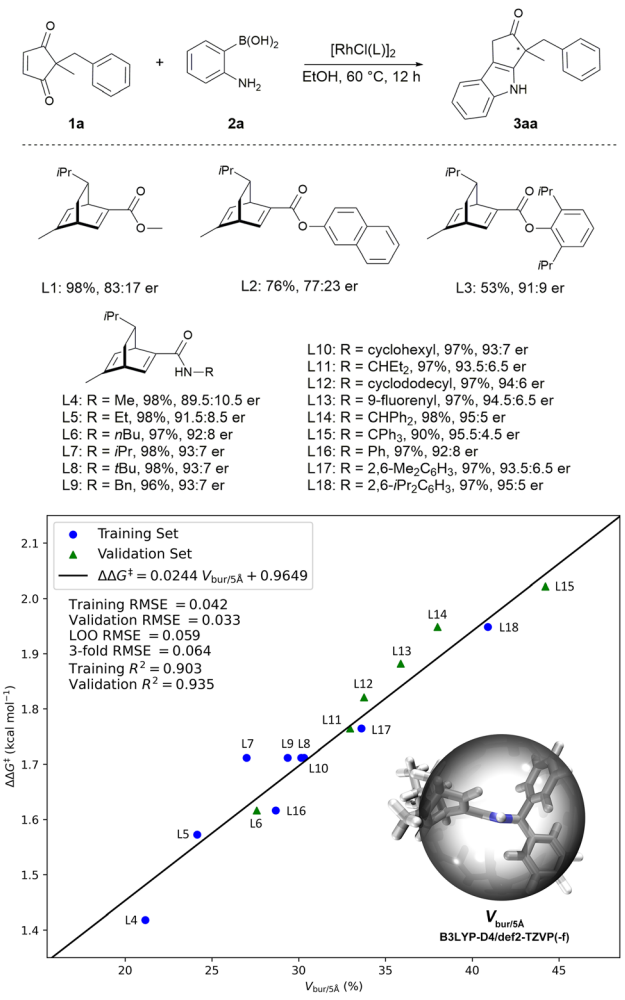

Scheme 2 Ligand optimization for the model asymmetric indolization reaction between cyclopentene-1,3-dione **1a** and 2-aminophenylboronic acid **2a**. Reaction conditions: **1a** (0.10 mmol), **2a** (0.20 mmol), and Rh catalyst (3 mol% Rh), in EtOH (1 mL) at 60 °C for 12 h. Yield was the isolated yield of **3aa**, and the er was determined by HPLC analysis on a chiral stationary phase. Measured $\Delta\Delta G^{\ddagger}$ were calculated using the formula $\Delta\Delta G^{\ddagger} = -RT\ln(er)$, where R is the ideal gas constant, and T is temperature.

Table 1 Further optimization of the reaction conditions[a]

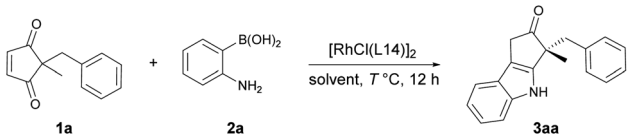

Entry	Solvent	T	Yield[b]	er[c]
1	EtOH	60	98	95 : 5
2	iPrOH	60	98	95 : 5
3	*t*BuOH	60	91	95 : 5
4	MeOH	60	98	92 : 8
5[d]	EtOH	60	81	93.5 : 6.5
6[e]	**EtOH**	**30/60**	**98**	96 : 4

[a] Reaction conditions: **1a** (0.10 mmol), **2a** (0.20 mmol), and Rh catalyst (3 mol% Rh), in the corresponding solvent (1 mL) at T °C for 12 h. [b] Isolated yield of **3aa**. [c] Determined by HPLC analysis on a chiral stationary phase. [d] Rh catalyst (1 mol% Rh) was used. [e] **1a** (0.10 mmol), **2a** (0.15 mmol), and Rh catalyst (3 mol% Rh), in EtOH (1 mL) at 30 °C for 12 h, then at 60 °C for 5 h.

amide in ligand and the measured Gibbs energy difference $\Delta\Delta G^{\ddagger}$ between two competing diastereomeric transition states (Scheme 2, training set). Leave-one-out (LOO) cross-validation and 3-fold cross-validation were implemented to avoid overfitting. Guided by this model, we synthesized ligands featuring different $V_{bur/5\ Å}$ (L6, L11, L12, L13, L14, L15) and tested their performances (Scheme 2, validation set). The newly synthesized ligands fitted well with the established model. Notably, ligand L15 featuring the largest percent buried volume exhibited the best enantiocontrol, however, it was not used for further study due to the lower reactivity. Pleasingly, ligands L14 and L18 proved to be optimal when considering both reactivity and enantioselectivity, and ligand L14 was selected for further investigation due to its easier preparation.

With ligand L14 in hand, further optimization was conducted to establish the optimal reaction conditions (Table 1). Similar yield and enantioselectivity were obtained when iPrOH was used instead of EtOH (entries 1 and 2). *t*BuOH led to a decreased yield (entry 3) while MeOH led to a diminished enantioselectivity (entry 4). Reducing the amount of catalyst to 1 mol% Rh slightly affected the yield and enantioselectivity (entry 5). When the reaction temperature was lowered, the conjugate addition reaction still proceeded well, but the subsequent intramolecular cyclization was not complete. Thus, the reaction was carried out successively at 30 °C and 60 °C to complete the conjugate addition and cyclization respectively, which further improved the enantioselectivity (entry 6, 96 : 4 er).

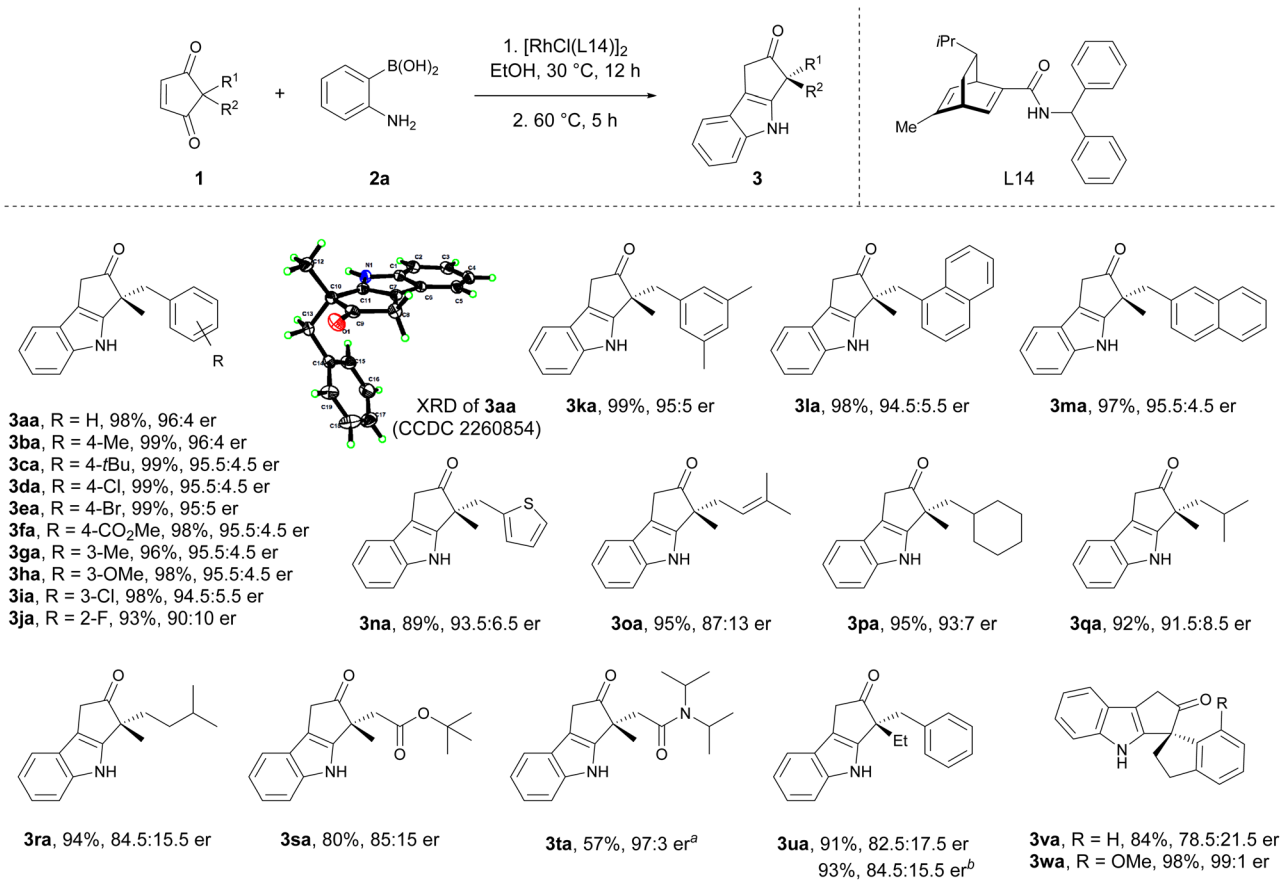

Scheme 3 The scope of 2,2-disubstituted cyclopentene-1,3-diones. Reaction conditions: **1** (0.20 mmol), **2a** (0.30 mmol), and Rh catalyst (3 mol% Rh), in EtOH (2 mL) at 30 °C for 12 h, then heating at 60 °C for 5 h. [a] Rh catalyst (8 mol% Rh) was used. [b] $[RhCl(L11)]_2$ was used as the catalyst.

With the optimal reaction conditions in hand, the scope of 2,2-disubstituted cyclopentene-1,3-diones for asymmetric indolization was explored (Scheme 3). Cyclopentene-1,3-diones substituted with methyl and various benzylic groups, including those with electron-donating and electron-withdrawing groups at *para*, *meta*, and *ortho* positions were all suitable (**3aa** to **3ka**). Replacement of the phenyl moiety with a naphthyl (**3la**, **3ma**) or a heteroaryl unit (**3na**) did not affect the reaction outcome. Cyclopentene-1,3-diones bearing allylic substituent (**3oa**) and different types of alkyl substituents (**3pa** to **3ra**) also exhibited good yields and high enantioselectivities. The ester and amide groups were tolerated (**3ra**, **3ta**), and the enantioselectivity for the bulky amide-containing substrate was much higher (85 : 15 er *versus* 97 : 3 er). The 2-ethyl-2-benzyl substituted substrate exhibited lower enantioselectivity (**3ua**) compared to its methyl congener (**3aa**), probably due to the diminished steric difference between the two substituents at 2-position. The spirocyclic substrates were also suitable for this reaction (**3va**, **3wa**). Notably, the 7-substituted spiroindane substrate gave the highest enantioselectivity (**3wa**, 99 : 1 er), which might be partially attributed to better enantio-face recognization induced by the rigid spiro structure and the substituent. The absolute configuration of **3aa** was determined by X-ray crystallography analysis, and the absolute configuration of other products was assigned by analogy.

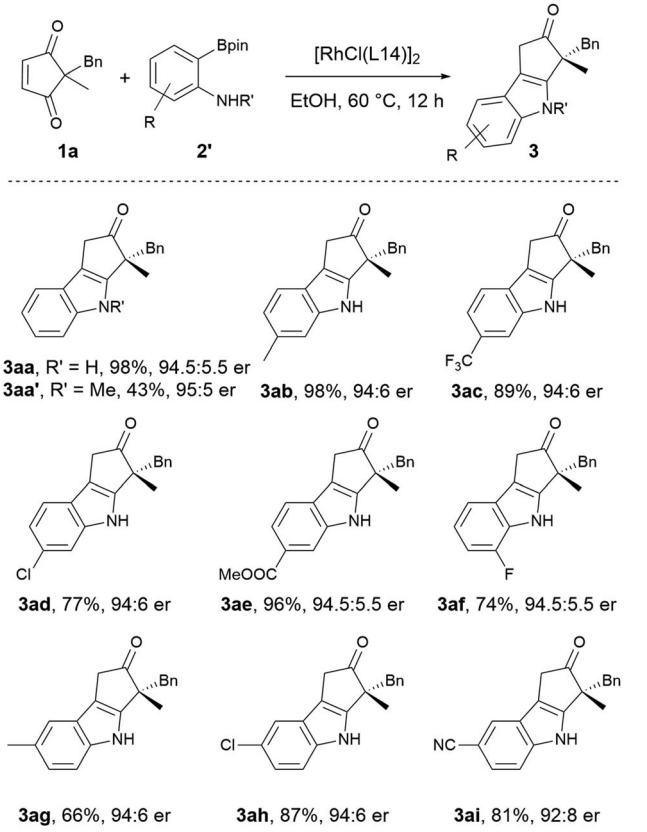

Scheme 4 The scope of 2-aminoarylboronic acid pinacol esters. Reaction conditions: **1a** (0.20 mmol), **2′** (0.30 mmol), and Rh catalyst (3 mol% Rh), in EtOH (2 mL) at 60 °C for 12 h.

The scope of 2-aminoarylborons was also explored. Although 2-aminophenylboronic acid is commercially available, other 2-aminoarylboronic acids are not readily accessible. Given the availability and well-established preparation of 2-aminoarylboronic acid pinacol esters,[21] they were employed for the scope study. It was found the pinacol esters exhibited lower reactivity at 30 °C, therefore the previously established conditions were slightly modified, and the reaction was conducted constantly at 60 °C. As shown in Scheme 4, the reaction using 2-aminophenylboronic acid pinacol ester proceeded smoothly to give the indolization product in 98% yield with 94.5 : 5.5 er (**3aa**), which is comparable to the optimal result from 2-aminophenylboronic acid. The *N*-methyl 2-aminophenylboronic acid pinacol ester was also tested under the standard conditions, and the *N*-methyl product was obtained in a moderate yield (43%) with a high enantioselectivity (95 : 5 er). The lower reactivity of the *N*-methyl reagent might be attributed to the lower reactivity of the corresponding bulkier arylrhodium species. All the other 2-aminoarylboronic acid pinacol esters bearing either electron-donating or electron-withdrawing substituents at different positions worked well to produce the substituted chiral indoles in high yields with good enantioselectivities (**3ab** to **3ai**). It is worth noting that the electron-withdrawing groups such as $-CF_3$ (**3ac**), $-CO_2Me$ (**3ae**), and –CN (**3ai**) are generally not well tolerated in the Fischer indolization, as they would result in diminished reactivity of the corresponding arylhydrazine substrates.[9]

A 2 mmol scale synthesis of product **3aa** was conducted to demonstrate the scalability of the asymmetric indolization reaction, and **3aa** could still be obtained in 98% yield with 95 : 5

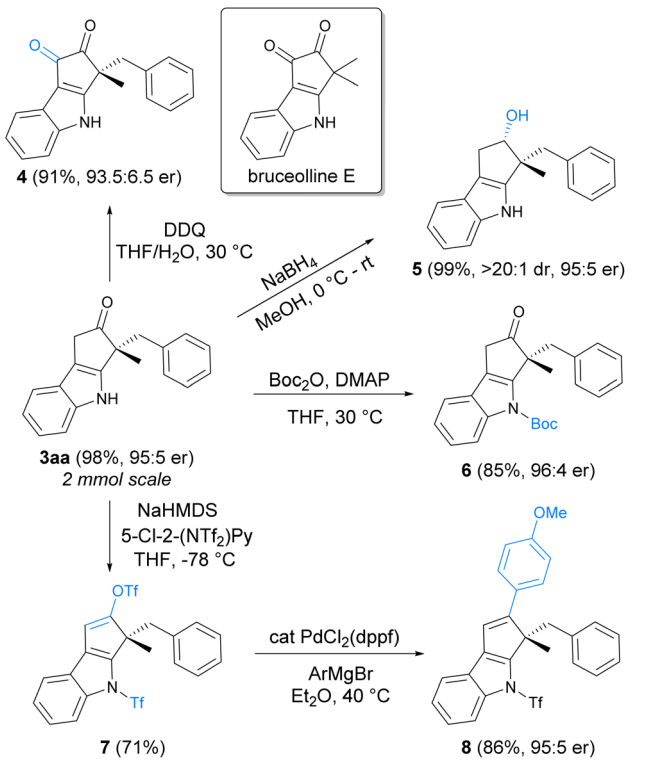

Scheme 5 Synthetic transformations of the chiral indole product.

er under standard conditions. Synthetic transformations of **3aa** to other indole derivatives were illustrated in Scheme 5. Oxidation of **3aa** with DDQ (2,3-dichloro-5,6-dicyano-1,4-benzoquinone) under mild conditions produced **4**, a chiral analogue of natural product bruceolline E featuring the cyclopenta[*b*]indole-1,2-dione core.[22] Reduction of the ketone moiety in **3aa** with $NaBH_4$ was highly effective, giving the chiral indole **5** bearing continuous quaternary–tertiary stereocenters in a highly diastereoselective manner. Protection of the free NH moiety with a Boc group could be performed under conventional conditions (**6**). In addition, conversion of the ketone to vinyl-OTf was viable (**7**), which could undergo Pd-catalyzed Kumada coupling to construct new carbon–carbon bond on the cyclopenta[*b*]indole ring (**8**).

To further explain the origin of enantioselectivity, we performed DFT calculations on the enantiocontrol step of the reaction (Fig. 1). We first identified the transition states for the enantioposition-selective alkene insertion step (with L8-ligated catalyst as a model), which was found to follow Hayashi's stereochemical model.[24] These transition states are stabilized by hydrogen bonding interactions between the N–H of the ligand and the carbonyl group of the substrate (see ESI-Section 6† for details). The surface distance projection maps of ligand–rhodium–substrate complex reflexed the relative spatial relationships between the substrate and the ligand.[25] For the transition state (TSDisf) leading to the unfavorable product, the benzyl group is closer to the ligand, and its rotation is hindered by the *tert*-butyl and methyl groups of the ligand. For the transition state (TSFav) leading to the favorable product, the rotation of the benzyl group is not affected, which has a more

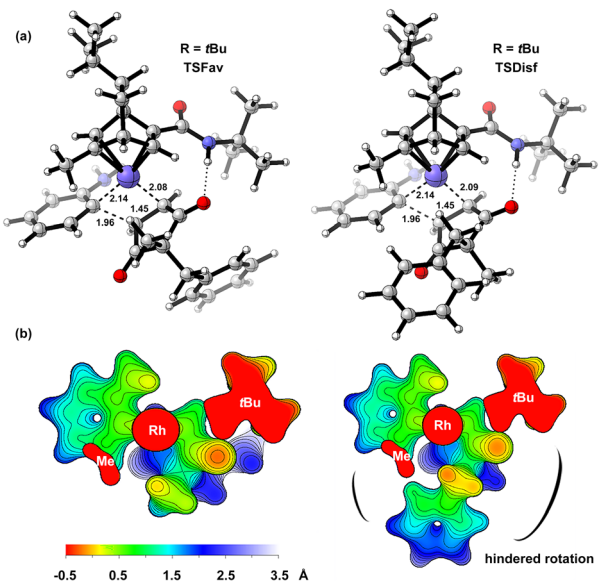

Fig. 1 The DFT model of transition states for the alkene insertion with L8-ligated catalyst (L8, R = *t*Bu) established at the SMD(ethanol)//PWPB95-D4/def2-TZVPP//C-PCM(ethanol)/PBE0-D4/def2-TZVP(for Rh)/def2-SVP (for other atoms) level.[23] (a) The optimized structures of transition states with $\Delta\Delta G_{TS}$ = 1.63 kcal mol^{-1} and er_{calc} = 92 : 8 (er_{exp} = 93 : 7). (b) The surface distance projection maps displayed from −0.5 Å to 3.5 Å centered on the rhodium atom.

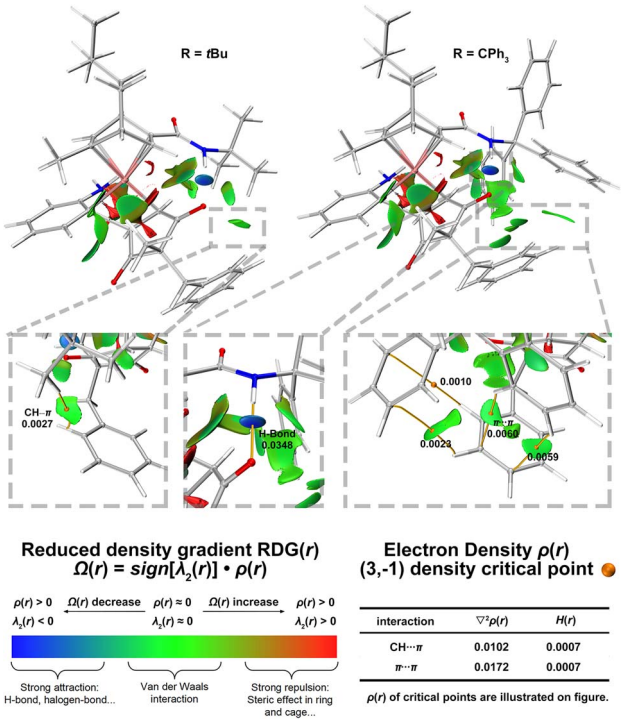

Fig. 2 The non-covalent interaction analysis within the sign(λ_2)ρ colored RDG plot and the topology analysis of the electron density within the framework of QTAIM for ligand L8 (R = *t*Bu) and L15 (R = CPh_3).

favorable entropy effect. The $\Delta\Delta G_{TS}$ is 1.63 kcal mol^{-1}, and the calculated er is in good agreement with the experimental result (er_{calc} = 92 : 8 *versus* er_{exp} = 93 : 7).

The non-covalent interaction analysis was also applied to transition states to understand the effect of the size of ligand substituent on enantioselectivity (Fig. 2).[26] In the favorable transition state of ligand L8 (R = *t*Bu), there is a CH···π interaction between *t*Bu and benzyl group. In the favorable transition state of ligand L15 (R = CPh_3), there are some π···π interactions between CPh_3 and benzyl group. The electron density $\rho(\boldsymbol{r})$, the Laplacian of electron density $\nabla^2\rho(\boldsymbol{r})$, and the energy density $H(\boldsymbol{r})$ of critical points also indicate these non-covalent interactions are van der Waals interactions which are usually dominated by dispersion effects.[27] These interactions are absent in the favorable transition state of ligand L4 (R = Me) as well as in those unfavorable transition states, thought to contribute greatly to the enantioselectivity (see ESI-Section 6† for details). As the size of the substituent on the ligand increases, its interactions with the benzyl group increase, leading to improved enantioselectivity.

Eyring analysis was also performed for different ligands (Table 2).[28] For ligand L4 (R = Me), the differential activation entropy $\Delta\Delta S^{\ddagger}$ is the factor dominating enantioselectivity. As we explained above, the rotation of the benzyl group in the unfavorable transition state is hindered, which is entropically unfavorable due to the steric repulsion of the ligand. For ligand L8 (R = *t*Bu) and ligand L14 (R = $CHPh_2$), the differential activation enthalpy $\Delta\Delta H^{\ddagger}$ becomes an increasingly important factor

Table 2 Eyring analysis[a]

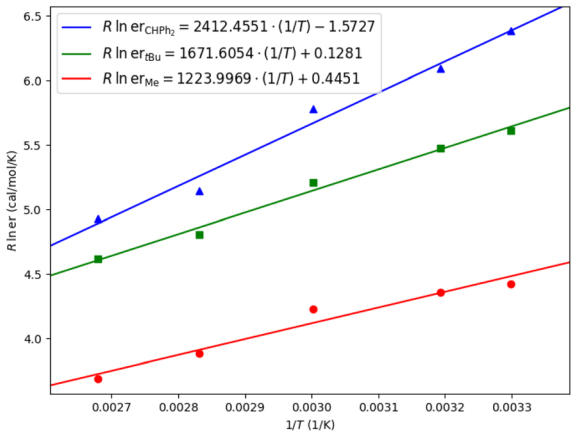

Entry	Ligand	$\Delta\Delta H^{\ddagger}$ (kcal mol^{-1})	$\Delta\Delta S^{\ddagger}$ (cal mol^{-1} K^{-1})
1	L4 (R = Me)	−1.224	0.445
2	L8 (R = *t*Bu)	−1.671	0.128
3	L14 (R = $CHPh_2$)	−2.412	−1.573

[a] Reaction conditions: **1a** (0.10 mmol), **2a** (0.20 mmol), and Rh catalyst (3 mol% Rh), in the EtOH (1 mL) at *T* °C for 12 h.

for enantiocontrol, which is consistent with our observation that there are additional non-covalent interactions in the favorable transition states. For L14, though the existence of enthalpy–entropy compensation reduces the favorable differential activation entropy $\Delta\Delta S^{\ddagger}$ to some extent, the significant favorable differential activation enthalpy $\Delta\Delta H^{\ddagger}$ greatly enhances the enantioselectivity.[29]

The role of amide–diene ligand in controlling enantioselectivity can be summarized as follows: (1) the rigid skeleton of the ligand provided steric repulsion to control the enantioselectivity, which is important in ligands with small substituents; (2) the amide moiety of the ligand provided hydrogen bonding interaction to stabilize the transition state; (3) the substituent moiety of the ligand provided dispersion interactions to stabilize the favourable transition state, which is important in ligands with large substituents.

Conclusions

In conclusion, we have developed a new type of asymmetric indolization reaction based on a desymmetrizing [3 + 2] annulation strategy, and a range of valuable cyclopenta[*b*]indoles bearing an all-carbon quaternary stereocenter were obtained in high yields with good enantioselectivities *via* a rhodium-catalyzed enantioposition-selective addition/5-*exo*-trig cyclization/dehydration cascade.[30] In this study, the optimal chiral ligand that can effectively control the formation of the remote stereocenter was identified based on a QSSR model, and further studies such as DFT calculation, non-covalent interaction analysis and Eyring analysis were performed to understand the multiple functions of the ligand.

Data availability

All experimental procedures, characterization, and computational details for this study can be found in the ESI.†

Author contributions

X. D. conceived the project. C. W. conducted the study under X. D.'s supervision. Z. C. conducted the initial investigation. C. P., C. B., and J. X. assisted with the experiments and the analytical characterization. C. W. performed the theoretical calculations and modelling. X. D. and C. W. wrote the manuscript. All authors discussed the results and commented on the manuscript.

Conflicts of interest

There are no conflicts to declare.

Acknowledgements

We thank the financial support from the Natural Science Foundation of Jiangsu Province (BK20200080) and the State Key Laboratory of Coordination Chemistry, Nanjing University. The authors thank the Hefei Advanced Computing Center for the computational resources.

Notes and references

1 (*a*) A. J. Kochanowska-Karamyan and M. T. Hamann, *Chem. Rev.*, 2010, **110**, 4489–4497; (*b*) N. K. Kaushik, N. Kaushik, P. Attri, N. Kumar, C. H. Kim, A. K. Verma and E. H. Choi, *Molecules*, 2013, **18**, 6620–6662; (*c*) T. V. Sravanthi and S. L. Manju, *Eur. J. Pharm. Sci.*, 2016, **91**, 1–10; (*d*) M. G. Ciulla and K. Kumar, *Tetrahedron Lett.*, 2018, **59**, 3223–3233; (*e*) Y. Wan, Y. Li, C. Yan, M. Yan and Z. Tang, *Eur. J. Med. Chem.*, 2019, **183**, 111691.

2 (*a*) U. Berens, J. M. Brown, J. Long and R. Selke, *Tetrahedron: Asymmetry*, 1996, **7**, 285–292; (*b*) T. Benincori, E. Brenna, F. Sannicol, L. Trimarco, P. Antognazz, E. Cesarotti, F. Demartin, T. Pilati and G. Zotti, *J. Organomet. Chem.*, 1997, **529**, 445–453; (*c*) T. Benincori, O. Piccolo, S. Rizzo and F. Sannicolò, *J. Org. Chem.*, 2000, **65**, 8340–8347; (*d*) T. Baumann and R. Brückner, *Angew. Chem., Int. Ed.*, 2019, **58**, 4714–4719; (*e*) T. He, L. Peng, S. Li, F. Hu, C. Xie, S. Huang, S. Jia, W. Qin and H. Yan, *Org. Lett.*, 2020, **22**, 6966–6971.

3 (*a*) G. Bartoli, G. Bencivenni and R. Dalpozzo, *Chem. Soc. Rev.*, 2010, **39**, 4449–4465; (*b*) R. Dalpozzo, *Chem. Soc. Rev.*, 2015, **44**, 742–778; (*c*) J.-B. Chen and Y.-X. Jia, *Org. Biomol. Chem.*, 2017, **15**, 3550–3567; (*d*) Y.-C. Zhang, F. Jiang and F. Shi, *Acc. Chem. Res.*, 2020, **53**, 425–446; (*e*) M.-S. Tu, K.-W. Chen, P. Wu, Y.-C. Zhang, X.-Q. Liu and F. Shi, *Org. Chem. Front.*, 2021, **8**, 2643–2672.

4 B.-M. Yang, X. Q. Ng and Y. Zhao, *Chem Catal.*, 2022, **2**, 3048–3076.

5 (*a*) N. Ototake, Y. Morimoto, A. Mokuya, H. Fukaya, Y. Shida and O. Kitagawa, *Chem.–Eur. J.*, 2010, **16**, 6752–6755; (*b*) L. Sun, H. Chen, B. Liu, J. Chang, L. Kong, F. Wang, Y. Lan and X. Li, *Angew. Chem., Int. Ed.*, 2021, **60**, 8391–8395; (*c*) Y. Wang, X. Zhou, W. Shan, R. Liao, Y. Deng, F. Peng and Z. Shao, *ACS Catal.*, 2022, **12**, 8094–8103; (*d*) Z.-S. Wang, L.-J. Zhu, C.-T. Li, B.-Y. Liu, X. Hong and L.-W. Ye, *Angew. Chem., Int. Ed.*, 2022, **61**, e202201436.

6 (*a*) L. Peng, K. Li, C. Xie, S. Li, D. Xu, W. Qin and H. Yan, *Angew. Chem., Int. Ed.*, 2019, **58**, 17199–17204; (*b*) Y.-P. He, H. Wu, Q. Wang and J. Zhu, *Angew. Chem., Int. Ed.*, 2020, **59**, 2105–2109; (*c*) W.-C. Yang, X.-B. Chen, K.-L. Song, B. Wu, W.-E. Gan, Z.-J. Zheng, J. Cao and L.-W. Xu, *Org. Lett.*, 2021, **23**, 1309–1314; (*d*) D. Xu, S. Huang, F. Hu, L. Peng, S. Jia, H. Mao, X. Gong, F. Li, W. Qin and H. Yan, *CCS Chem.*, 2022, **4**, 2686–2697.

7 (*a*) M. Tian, D. Bai, G. Zheng, J. Chang and X. Li, *J. Am. Chem. Soc.*, 2019, **141**, 9527–9532; (*b*) S. Lu, J.-Y. Ong, H. Yang, S. B. Poh, X. Liew, C. S. D. Seow, M. W. Wong and Y. Zhao, *J. Am. Chem. Soc.*, 2019, **141**, 17062–17067; (*c*) C.-S. Wang, L. Wei, C. Fu, X.-H. Wang and C.-J. Wang, *Org. Lett.*, 2021, **23**, 7401–7406; (*d*) X. Li, L. Zhao, Z. Qi and X. Li, *Org. Lett.*, 2021, **23**, 5901–5905; (*e*) S. Jia, Y. Tian, X. Li, P. Wang, Y. Lan and H. Yan, *Angew. Chem., Int. Ed.*, 2022, **61**, e202206501; (*f*) H. Yang, H.-R. Sun, R.-Q. He, L. Yu, W. Hu, J. Chen, S. Yang, G.-G. Zhang and L. Zhou, *Nat. Commun.*, 2022, **13**, 1–9.

8 (*a*) K.-W. Chen, Z.-H. Chen, S. Yang, S.-F. Wu, Y.-C. Zhang and F. Shi, *Angew. Chem., Int. Ed.*, 2022, **61**, e202116829; (*b*) P. Zhang, Q. Xu, X.-M. Wang, J. Feng, C.-J. Lu, Y. Li and R.-R. Liu, *Angew. Chem., Int. Ed.*, 2022, **61**, e202212101; (*c*) Z.-H. Chen, T.-Z. Li, N.-Y. Wang, X.-F. Ma, S.-F. Ni, Y.-C. Zhang and F. Shi, *Angew. Chem., Int. Ed.*, 2023, **62**, e202300419; (*d*) L.-Y. Wang, J. Miao, Y. Zhao and B.-M. Yang, *Org. Lett.*, 2023, **25**, 1553–1557.

9 (*a*) S. Müller, M. J. Webber and B. List, *J. Am. Chem. Soc.*, 2011, **133**, 18534–18537; (*b*) A. Martínez, M. J. Webber, S. Müller and B. List, *Angew. Chem., Int. Ed.*, 2013, **52**, 9486–9490; (*c*) L. Kötzner, M. J. Webber, A. Martínez, C. De Fusco and B. List, *Angew. Chem., Int. Ed.*, 2014, **53**, 5202–5205; (*d*) B. Ghosh, R. Balhara, G. Jindal and S. Mukherjee, *Angew. Chem., Int. Ed.*, 2021, **60**, 2–9.

10 (*a*) J. Chen, X. Han and X. Lu, *Angew. Chem., Int. Ed.*, 2017, **56**, 14698–14701; (*b*) Y.-P. He, J. Cao, H. Wu, Q. Wang and J. Zhu, *Angew. Chem., Int. Ed.*, 2021, **60**, 7093–7097; (*c*) A. Whyte, J. Bajohr, R. Arora, A. Torelli and M. Lautens, *Angew. Chem., Int. Ed.*, 2021, **60**, 20231–20236; (*d*) G. Yang, J. Pan, Y.-M. Ke, Y. Liu and Y. Zhao, *Angew. Chem., Int. Ed.*, 2021, **60**, 20689–20694; (*e*) G. Wang, J.-C. Li, Y.-G. Zhou and Z.-S. Ye, *Org. Lett.*, 2021, **23**, 802–807; (*f*) X.-D. Hu, Z.-H. Chen, J. Zhao, R.-Z. Sun, H. Zhang, X. Qi and W.-B. Liu, *J. Am. Chem. Soc.*, 2021, **143**, 3734–3740.

11 During the preparation of this manuscript, a copper-catalyzed asymmetric radical cascade reaction reaction was disclosed by Leifert and Studer group to realize the asymmetric Fukuyama indole synthesis, see: T. Drennhaus, D. Leifert, J. Lammert, J. P. Drennhaus, K. Bergander, C. G. Daniliuc and A. Studer, *J. Am. Chem. Soc.*, 2023, **145**, 8665–8676.

12 J. Li and J. M. Cook in *Name Reactions in Heterocyclic Chemistry*, ed. J. J. Li, Wiley, Hoboken NJ, 2005, pp. 154–158.

13 (*a*) X. Dou, Y. Huang and T. Hayashi, *Angew. Chem., Int. Ed.*, 2016, **55**, 1133–1137; (*b*) L. Yin, J. Xing, Y. Wang, Y. Shen, T. Lu, T. Hayashi and X. Dou, *Angew. Chem., Int. Ed.*, 2019, **58**, 2474–2478; (*c*) B. Ye, J. Yao, C. Wu, H. Zhu, W. Yao, L. Jin and X. Dou, *ACS Catal.*, 2022, **12**, 2434–2440.

14 (*a*) T. Yasukawa, H. Miyamura and S. Kobayashi, *Acc. Chem. Res.*, 2020, **53**, 2950–2963; (*b*) M. M. Heravi, M. Dehghani and V. Zadsirjan, *Tetrahedron: Asymmetry*, 2016, **27**, 513–588; (*c*) P. Tian, H.-Q. Dong and G.-Q. Lin, *ACS Catal.*, 2012, **2**, 95–119; (*d*) T. Hayashi and K. Yamasaki, *Chem. Rev.*, 2003, **103**, 2829–2844; (*e*) K. Fagnou and M. Lautens, *Chem. Rev.*, 2003, **103**, 169–196.

15 (*a*) J. Horn, S. P. Marsden, A. Nelson, D. House and G. G. Weingarten, *Org. Lett.*, 2008, **10**, 4117–4120; (*b*) H. Y. Li, J. Horn, A. Campbell, D. House, A. Nelson and S. P. Marsden, *Chem. Commun.*, 2014, **50**, 10222–10224; (*c*) H. Lam, J. Tsoung and M. Lautens, *J. Org. Chem.*, 2017, **82**, 6089–6099.

16 T. Das, *ChemistrySelect*, 2020, **5**, 14484–14509.

17 X.-P. Zeng, Z.-Y. Cao, Y.-H. Wang, F. Zhou and J. Zhou, *Chem. Rev.*, 2016, **116**, 7330–7396.

18 Y. Huang and T. Hayashi, *Chem. Rev.*, 2022, **18**, 14346–14404.

19 (*a*) G. Pattison, G. Piraux and H. W. Lam, *J. Am. Chem. Soc.*, 2010, **132**, 14373–14375; (*b*) I. D. Roy, A. B. Burns, G. Pattison, B. Michel, A. J. Parker and H. W. Lam, *Chem. Commun.*, 2014, **50**, 2865–2868; (*c*) M. Hatano and T. Nishimura, *Angew. Chem., Int. Ed.*, 2015, **127**, 11099–11102; (*d*) F. Xue and T. Hayashi, *Angew. Chem., Int. Ed.*, 2018, **57**, 10368–10372.

20 For the pioneering work and reviews on quantitative structure–selectivity relationship, see: (*a*) K. C. Harper and M. S. Sigman, *Proc. Natl. Acad. Sci. U. S. A.*, 2011, **108**, 2179–2183; (*b*) A. F. Zahrt, S. V. Athavale and S. E. Denmark, *Chem. Rev.*, 2020, **120**, 1620–1689; (*c*) J. M. Crawford, C. Kingston, F. D. Toste and M. S. Sigman, *Acc. Chem. Res.*, 2021, **54**, 3136–3148; (*d*) W. L. Williams, L. Zeng, T. Gensch, M. S. Sigman, A. G. Doyle and E. V. Anslyn, *ACS Cent. Sci.*, 2021, **7**, 1622–1637.

21 (*a*) M. R. Smith III, R. Bisht, C. Haldar, G. Pandey, J. E. Dannatt, B. Ghaffari, R. E. Maleczka Jr and B. Chattopadhyay, *ACS Catal.*, 2018, **8**, 6216–6223; (*b*) S. M. Preshlock, D. L. Plattner, P. E. Maligres, S. W. Krska, R. E. Maleczka Jr and M. R. Smith III, *Angew. Chem., Int. Ed.*, 2013, **52**, 12915–12919.

22 J. M. Lopchuk, I. L. Green, J. C. Badenock and G. W. Gribble, *Org. Lett.*, 2013, **15**, 4485–4487.

23 (*a*) F. Neese, *Wiley Interdiscip. Rev.: Comput. Mol. Sci.*, 2018, **8**, e1327; (*b*) F. Neese, *Wiley Interdiscip. Rev.: Comput. Mol. Sci.*, 2022, **12**, e1606; (*c*) T. Lu and F. Chen, *J. Comput. Chem.*, 2012, **33**, 580–592.

24 For more information on Hayashi's stereochemical model, see: (*a*) G. Berthon and T. Hayashi in *Catalytic Asymmetric Conjugate Reactions*, ed. A. Córdova, Wiley-VCH Verlag

GmbH & Co. KGaA, Weinheim, 2010, pp. 1–70; (*b*) E. A. B. Kantchev, *Chem. Sci.*, 2013, **4**, 1864–1875.

25 For the pioneering work on surface distance projection maps, see: (*a*) A. Poater, F. Ragone, R. Mariz, R. Dorta and L. Cavallo, *Chem.–Eur. J.*, 2010, **16**, 14348–14353; (*b*) L. Falivene, R. Credendino, A. Poater, A. Petta, L. Serra, R. Oliva, V. Scarano and L. Cavallo, *Organometallics*, 2016, **35**, 2286–2293; (*c*) L. Falivene, Z. Cao, A. Petta, L. Serra, A. Poater, R. Oliva, V. Scarano and L. Cavallo, *Nat. Chem.*, 2019, **11**, 872–879.

26 For the pioneering work and reviews on non-covalent interaction analysis and topology analysis, see: (*a*) E. R. Johnson, S. Keinan, P. Mori-Sánchez, J. Contreras-García, A. J. Cohen and W. Yang, *J. Am. Chem. Soc.*, 2010, **18**, 6498–6506; (*b*) R. Laplaza, F. Peccati, R. A. Boto, C. Quan, A. Carbone, J.-P. Piquemal, Y. Maday and J. Contreras-García, *Wiley Interdiscip. Rev.: Comput. Mol. Sci.*, 2020, **11**, e1497; (*c*) R. F. W. Bader, *Atoms in molecules: a quantum theory*, Clarendon Press, Oxford, 1994, pp. 1–432; (*d*) P. L. A. Popelier in *The Chemical Bond: Fundamental aspects of chemical bonding*, ed. G. Frenking and S. Shaik, Wiley-VCH Verlag GmbH & Co. KGaA, Weinheim, 2010, pp. 271–308.

27 For reviews on dispersion effects, see: (*a*) J. P. Wagner and P. R. Schreiner, *Angew. Chem., Int. Ed.*, 2015, **54**, 12274–12296; (*b*) M. Stöhr, T. V. Voorhisb and A. Tkatchenko, *Chem. Soc. Rev.*, 2019, **48**, 4118–4154; (*c*) K. L. Mears and P. P. Power, *Acc. Chem. Res.*, 2022, **55**, 1337–1348.

28 For the pioneering work and reviews on Eyring analysis, see: (*a*) M. Palucki, N. S. Finney, P. J. Pospisil, M. L. Güler, T. Ishida and E. N. Jacobsen, *J. Am. Chem. Soc.*, 1998, **120**, 948–954; (*b*) R. R. Knowles, S. Lin and E. N. Jacobsen, *J. Am. Chem. Soc.*, 2010, **132**, 5030–5032; (*c*) E. V. Anslyn and D. A. Dougherty, *Modern Physical Organic Chemistry*, University Science Books, United States of America, 2006, pp. 370–372.

29 For reviews on enthalpy–entropy compensation, see: (*a*) W. Linert, *Chem. Soc. Rev.*, 1994, **23**, 429–438; (*b*) L. Liu and Q.-X. Guo, *Chem. Rev.*, 2001, **101**, 673–696; (*c*) A. Pan, T. Biswas, A. K. Rakshit and S. P. Moulik, *J. Phys. Chem. B*, 2015, **119**, 15876–15884.

30 Two other pathways, *i.e.*, rhodium-catalyzed enantioposition-selective imine formation/Rh-catalyzed intramolecular addition/isomerization pathway or reversable imine formation/Rh-catalyzed dynamic kinetic intramolecular addition/isomerization pathway, are unlikely but not impossible. These pathways could not be ruled out at this stage.